DOI: 10.1002/ejic.201000966

A Clean Low-Temperature ZnO Deposition Method for Multipurpose Applications

Marc Estruga,*[a] Irene Gonzalez-Valls,[b] Concepción Domingo,[c] Monica Lira-Cantu,[b] and José A. Ayllón*[a]

Keywords: Nanostructures / Semiconductors / Energy conversion / Zinc oxide / Low-temperature deposition

Zinc oxide (ZnO) was dissolved in an aqueous solution of ammonia and hydrogen peroxide. According to XRD characterization, this precursor solution yielded crystalline zinc oxide after evaporation and thermal treatment at 90 °C for 2 h. The processability of this precursor solution allowed for ZnO deposition on cellulose paper, which is an example of a thermolabile substrate. Cellulose filter paper that was impregnated with this solution and subsequently thermally treated at 90 °C for 2 h had nanostructured crystalline ZnO well adhered to its surface. This composite material was characterized by XRD and scanning electron microscopy (SEM). The described precursor solution also assisted in the preparation of ZnO porous layers for dye-sensitized solar cells (DSC). For this purpose, it was mixed with ZnO nanopowder dispersed in ethanol. The mixture was then sprayed on transparent conductive oxide substrates. In this way porous films were obtained after heat treatment at 90 °C for 2 h. Under standard testing conditions (AM1.5G, 100 mW cm^{-2}), a device prepared with $(Bu_4N)_2[Ru(dcbpyH)_2(NCS)_2]$ (dcbpy = 4,4′-dicarboxy-2,2′-bipyridine) (N-719) dye and a film thickness of 5 μm exhibited 1.43 % efficiency.

Introduction

ZnO is a technologically valuable semiconductor that has attracted considerable attention because of its excellent catalytic, electrical and optical properties.[1–4] Consequently, several physical and chemical methods have been explored for the deposition of zinc oxide with different morphologies on a myriad of substrates.[5,6] Indeed, considerable research effort is focused on low-temperature and clean ZnO deposition methods,[7–12] with a second objective of developing a synthetic route that will be compatible with thermolabile substrates while minimizing energy consumption.

In this context, zinc peroxide (ZnO_2) is a clean precursor that yields, by thermal treatment, ZnO free of impurities since molecular oxygen is the only by-product of its decomposition. However, ZnO_2 is insoluble in common solvents, therefore it has been either grown directly onto different substrates by the chemical bath deposition (CBD) method[7,13] or added by electrodeposition.[14] Post-deposition thermal treatment at 180–230 °C is required for the conversion of the as-deposited material to ZnO. Thus, this route is not compatible with thermolabile substrates such as polymers or organic fibers that cannot withstand such high temperatures.

CBD with other precursors has been widely explored as an alternative means for the production of ZnO films.[15,16] This technology presents many advantages such as low-temperature and ambient-pressure processing, low cost chemical precursors, unsophisticated apparatus, uniform deposits, etc. Nevertheless, CBD cannot be easily incorporated into automatic continuous fabrication processes, and the maintenance, depuration and disposal of the bath solution are also important issues that need to be addressed.

Solution processing of any material is highly desirable from an energy efficiency point of view.[17] Moreover, precursors that decompose at low temperatures to give pure materials that are free of undesirable by-products are required for nanotechnology applications. However, solutions for CBD technology cannot be used for simpler processes such as spray, ink-jet or dipping methods that require the precursor solution to evaporation to dryness, since these solutions would lead to undesirable mixtures of compounds.

ZnO films can also be deposited from preformed organic-capped ZnO nanoparticles by taking advantage of their good dispersibility in organic solvents. For example, deposition of ZnO nanoparticles with volatile amines as capping agents, e.g. butylamine, which were eliminated overnight by vacuum treatment, allowed for the low-temperature sintering of the precursor solution to produce nanostructured ZnO films.[18] The development of a low-

[a] Departament de Química, Universitat Autònoma de Barcelona, Campus UAB,
08193 Bellaterra, Spain
Fax: +34-93-581-2920
E-mail: joseantonio.ayllon@uab.es
mestruga@qf.uab.cat
[b] Centre d'Investigació en Nanociència i Nanotecnologia (CIN2, CSIC-ICN), Campus UAB,
08193 Bellaterra, Spain
[c] Institut de Ciència dels Materials de Barcelona (CSIC), Campus UAB,
08193 Bellaterra, Spain

temperature and substrate-friendly method for the fabrication of ZnO thin films is of great importance for photovoltaic technology, where ZnO is a component of inorganic,[19] dye-sensitized[20,21] and organic solar cells.[22–25]

Of special relevance is the utilization of synthesis methods where no residue of any kind is left after ZnO preparation, since it is well known that the optical properties of ZnO are modified by the presence of even traces amounts of impurities.[26–29] As such impurities have been proven to modify not only the performance of solar cells,[30] but also other optoelectronic devices like organic light-emitting diodes (OLEDs)[31,32] and field-effect transistors.[27,28] On the other hand, the deposition of ZnO nanoparticles on the pores of paper and other cellulose based materials, such as wood or cotton, could have potential application in systems for UV light barriers, antibacterial activity, strain sensors, etc.[33–38]

In this work, we describe the preparation of an aqueous ZnO precursor solution that neatly decomposes after evaporation and short thermal treatment at 90 °C. The developed method facilitates the deposition and sintering of crystalline ZnO materials at a temperature that is compatible with thermolabile substrates. The usefulness of the new precursor solution for the low-temperature preparation of porous ZnO films has also been proven. Such films are of interest as potential photoanodes for DSCs.

Results and Discussion

1.1 Precursor Solution

Simple preliminary essays were conducted by dissolving ZnO in aqueous ammonia. Due to its high coordination affinity with Zn^{II}, NH_3 is a good stabilizing agent for this cation, it also has the advantage of being highly volatile. However, the solubility of the ZnO was limited to about 3500 mg L^{-1}, even in concentrated ammonia. It has been reported that freshly precipitated zinc hydroxide is much more soluble in aqueous ammonia that zinc oxide.[39] However, the use of zinc hydroxide was discarded because this reagent is unstable and difficult to purify.[40] Our research then focused on the use of additives that will increase the solubility of ZnO in aqueous ammonia, and which are labile enough to be eliminated after evaporation to dryness at a low temperature. Satisfactory results were obtained with hydrogen peroxide at a relatively low concentration (ca. 0.37 M); with this as the additive, solutions containing 12000 mg L^{-1} of ZnO could be obtained rapidly.

The increase in ZnO solubility after the addition of hydrogen peroxide to the solution could be related to equilibrium displacement due to the weak acidic character of this compound:

$$ZnO + 4NH_3 + H_2O \leftrightarrows [Zn(NH_3)_4]^{2+} + 2OH^-$$

$$OH^- + H_2O_2 \leftrightarrows H_2O + HO_2^-$$

XRD characterization of the dry residue obtained after evaporation at room temperature (Figure 1, a) revealed that the as-prepared material mainly constituted crystalline ZnO (wurtzite, ICDD 79-2205). Some of the less intense peaks in the pattern were assigned to $Zn(OH)_2$ (solid triangles at 27.56° and 38.88°). After raising the evaporation temperature to 50 °C, the amount of impurities in the residue diminished (Figure 1, b). Finally, evaporation and thermal treatment at 90 °C completely eliminated impurities from the residue; XRD showed that the obtained material is composed of crystalline ZnO (Figure 1, c). The ZnO particle size was estimated to be approx. 30 nm (according to the Scherrer equation applied to the 100 peak). Moreover, infrared spectroscopy showed that only small amounts of carbonate residues are present after thermal treatment, a common occurrence for ZnO-based materials.[41,42]

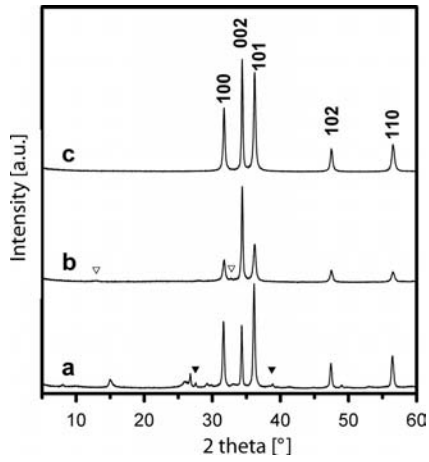

Figure 1. Powder XRD characterization of the residues obtained after overnight evaporation of the precursor solution at room temperature (a); overnight evaporation at 50 °C (b); evaporation at 90 °C for 2 h (c). Wurtzite patterns are indexed for comparison purposes (ICDD number 79-2205). $Zn(OH)_2$ residue peaks appeared at 2θ = 27.56 and 38.88° after room temperature evaporation (solid triangles). Unidentified impurities remained after the treatement at 50 °C (open triangles).

1.2 ZnO Deposition on Cellulose

To demonstrate the applicability of the described aqueous ZnO precursor solution, a standard filter paper composed of cellulose fibers was selected as thermolabile substrate. Following the impregnation method described in the Experimental section, the loading of ZnO could be adjusted by varying the amount of precursor solution added to the substrate. After evaporation to dryness and thermal treatment at 90 °C for 2 h, XRD characterization showed that crystalline nanosized ZnO was produced (Figure 2). The relatively broad ZnO peaks in the pattern (see Figure 1, c and Figure 2, b) demonstrated that, in this case, the presence of multiple nucleation sites on the substrate surface led to a reduction in the ZnO crystallite size (to about 13 nm, according to the Scherrer equation applied to the 100 peak). The nano ZnO coated paper was sonicated for 5 min while immersed in water, and no noticeable ZnO detachment was observed by UV/Vis spectroscopy. Hence, neither pretreatment nor the use of binders is necessary to obtain a stable

deposit. The dried composite was analyzed by SEM (Figure 3). The SEM micrographs revealed the formation of ZnO deposits on the cellulose fibers. Moreover, the external surface fibers are almost completely covered, while discontinuous deposits are observed on the interior surfaces. A closer view of the deposits shows the formation of cauliflower-shaped aggregates that are formed at the spaced nucleation sites, and are indicated by the presence of multiple nanocrystals (Figure 3, c).

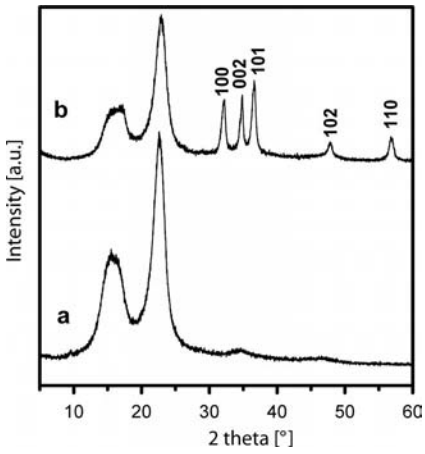

Figure 2. XRD pattern of the filter paper substrate: before deposition (a), and after ZnO deposition (b). Wurtzite patterns are indexed for comparison purposes (ICDD n° 79–2205).

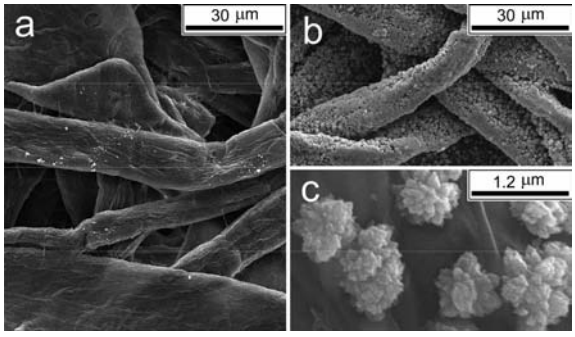

Figure 3. SEM micrographs of the filter paper substrate: before deposition (a), and after ZnO deposition (b), and after deposition and 5 min of sonication treatment (c).

1.3 Dye-Sensitized Solar Cells

The aqueous precursor solution has also been used to connect preformed ZnO nanoparticles at low temperature, and avoiding a high temperature sintering step. In this way porous ZnO films useful for DSC applications were obtained. In the first step, a blocking layer of ZnO nanoparticles (100 nm thick) was spin-coated onto the top of fluorine-doped tin oxide (FTO) substrates. Then, ZnO porous layers were applied to the surface of the substrate by spray coating it with a mixture of commercial ZnO nanoparticles and the ZnO precursor solution detailed above. The ZnO nanopowder was first suspended in ethanol, and the soluble precursor was added in the necessary proportion to yield 10 wt.-% of oxide after its transformation to ZnO. During the thermal treatment (90 °C for 2 h), crystallization of ZnO from the precursor solution occurred, assuring the connection of the particles and providing self-consistency to the film. Control films that were deposited on bare glass or plastic, detached from these substrates in the form of sheet pieces that were several square mm in area, suggesting that the sintering process was very effective, and confirmed that ZnO sintering was achieved at the low temperature of 90 °C. On the other hand, sprayed films comprising commercial ZnO, in absence of precursor solution, had poor self-consistency and bad adherence to the substrate.

SEM micrographs confirmed the porous structure of the film (Figure 4) where the morphology of the commercial ZnO prevailed, suggesting that the additional ZnO material obtained from the precursor solution acted as a connecting agent for the powder particles. This feature is highly desirable for DSC applications, since the amount of dye adsorption (and thus, photocurrent) is directly proportional to the surface area of the film. In fact, the specific surface area of the film was estimated by nitrogen sorption analysis to be 13 $m^2 g^{-1}$.

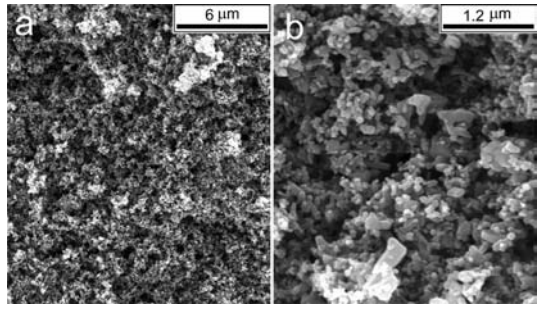

Figure 4. SEM micrographs of the porous ZnO layer for DSC before dye adsorption.

The absorption isotherm shape and the pore size distribution analysis of the film (Figure 5) denoted the presence of pores that are about 100 nm in size (inset, plot a) and could be related to interaggregate pores, which are easily accessible for dye adsorption. DSC characterization indicated that the mixture yielded reasonably good results under standard test conditions (AM1.5G, 100 mW cm^{-2}). The best performance obtained among several cells of 5 µm thickness with an active area of 0.159 cm^2 showed the following working parameters (Figure 6): V_{oc} = 737 mV; J_{sc} = 3.53 mA cm^{-2}; FF = 0.55, which yields a global efficiency (η) of 1.43%. This performance is lower than the reported values for other low-temperature ZnO DSCs,[43] but it has to be considered than expensive treatments, like high vacuum steps, have been avoided in this work. Moreover, incident photon-to-current efficiency (IPCE) reached a maximum of 8% at 530 nm (Figure 6, inset), which indicates that the dye injection is somehow restricted in this system. A possible reason for this could be the open porous film structure, although it enhances the dye adsorption capacity, it could also hinder electron transport from the excited dye to the FTO collector.[44] Thus, despite the DSC fabrication

process and parameters that effect the cell efficiency not being optimized, these results show that the proposed precursor solution may have prospective application in the low-temperature manufacture of such devices.

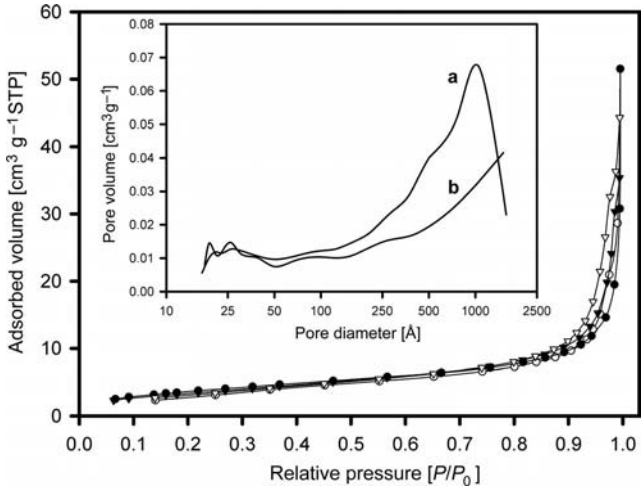

Figure 5. Nitrogen sorption analysis of the porous ZnO layer in a DSC (triangles) compared with a commercial ZnO nanopowder (circles). Inset: pore size distributions calculated from the adsorption branches of the isotherms: porous ZnO layer in a DSC (a) and commercial ZnO nanopowder (b).

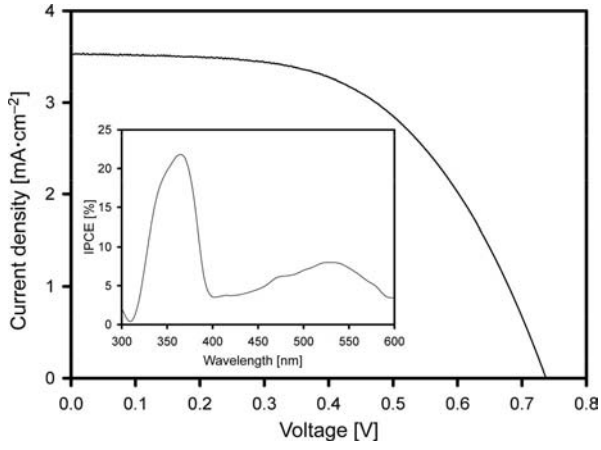

Figure 6. JV curves obtained for representative DSC devices. Inset: IPCE action spectra.

Conclusions

The usefulness of a user-friendly ZnO precursor, based on an aqueous solution containing ammonia and hydrogen peroxide, was demonstrated. Hydrogen peroxide acted as a weak acid, increasing the ZnO solubility. The subsequent ammonia evaporation and short thermal treatment at 90 °C led to anion-free ZnO nanopowders. This clean low-temperature approach has been used to deposit ZnO on filter paper, a thermo labile substrate. Moreover, the feasibility of the method for the preparation of porous ZnO layers for DSCs has also been explored, with the precursor solution acting as a connecting agent for commercial ZnO nanopowders. The ZnO DSC devices prepared at low temperature by this method exhibited a maximum efficiency of 1.43% under standard test conditions, a reasonably good performance considering that neither vacuum nor high temperature treatments were applied in their fabrication.

Experimental Section

Materials: All chemicals used in this work were commercially available and were used without further purification: ZnO nanopowder (< 100 nm, 99.5 wt.-%, ref. 544906 Sigma–Aldrich), ammonia (30 wt.-% in water, Panreac), hydrogen peroxide (33% w/v in water, Panreac), ethanol (99.5%, Panreac), ultra pure water (Milli-Q system, conductivity lower than 0.05 μScm^{-1}). Standard laboratory filter paper, composed basically of cellulose fibers, was used as a model thermolabile substrate (Paper reams, ref. 2504252, Albet). FTO 2.5×1 cm^2 slides were purchased from Solems (R = 70–100 Ω, FTO layer produced by magnetron sputtering with a thickness of 800 Å on glass, 1 mm thickness). The electrolyte Iodolyte AN-50, the N-719 dye, the Pt paste, Pt catalyst T/SP and the hot melt sealing foil (SX1170), were all purchased from Solaronix.

Precursor Solution Preparation: In a closed polytetrafluoroethylene (PTFE) container, ZnO nanopowder (600 mg) was added to a commercial aqueous ammonia solution (50 mL), giving a white powder suspension. Subsequently, a commercial solution of hydrogen peroxide (2 mL) was added whilst the mixture was stirred and a stable clear transparent solution was immediately obtained (the ZnO concentration was about 12 $g L^{-1}$). The precursor solution decomposition was conducted with a hot plate at room temperature, 50 °C and 90 °C, and the phase composition of the resultant films were examined by XRD.

Deposition on Cellulose: A piece of standard filter paper (3×4 cm^2) was accurately weighted (86.3 mg) and impregnated with precursor solution (1.44 mL) to obtain a composite with a 20 wt.-% of ZnO. The impregnation process was divided into seven steps to assure homogeneous distribution of the ZnO inside the cellulose. Subsequently, the paper was heated at 90 °C for 2 h in a forced air circulation oven. The as-prepared coated paper was immersed in water and sonicated for 5 min to evaluate the adherence of the ZnO nanoparticles to the paper. No detached particles were observed and the possibility of nanoparticles remaining in suspension was ruled out by UV/Vis spectroscopic analysis.

Solar Cell Fabrication: FTO slides (2.5×1 cm^2) were consecutively washed, while being sonicated, with detergent (Empigem BB, Aldrich), ultra pure water and ethanol, and then dried under N_2 flux, and finally cleaned for 20 min in a UV-surface decontamination system (Novascan, PSD-UV) connected to an oxygen gas source. Subsequently, a compact layer (100 nm thick) of ZnO nanoparticles was deposited on the slides by spin coating at 1000 rpm to avoid direct electrolyte reaction over the FTO substrate. The as-prepared precursor solution (10 mL) was mixed with commercial ZnO nanopowder (1.2 g) and ethanol (10 mL), and the obtained suspension was sprayed over the prepared substrates with an airbrush. After spray deposition, thermal treatment was conducted at 90 °C for 2 h, yielding the porous ZnO layer. The FTO/ZnO substrates were then immersed, while hot, in a 0.5 mM ethanol solution of N-719 dye (Solaronix) for 16 h at room temperature in the dark. The effective area of the cell was 0.159 cm^2. The counter electrode was platinized FTO, and the DSCs were thermally sealed with hot melt sealing foil as a spacer. A vacuum was applied to introduce the

electrolyte by capillary force and the filling holes were then immediately sealed with small pieces of glass.

Characterization: XRD spectra were recorded on a Rigaku Rotaflex RU-200B diffractometer with Cu-$K_{\alpha 1}$ radiation (λ = 1.5406 Å). SEM images were recorded with a Hitachi S-570 microscope operating at 20 kV. Textural properties of the porous ZnO layer were studied by low-temperature N_2 sorption analysis (ASAP 2000 Micromeritics). Prior to measurements, samples were dried under reduced pressure (<1 mPa) at 393 K for 18 h. Specific surface area (Sa) values were determined from the adsorption branch of the isotherms by the BET method.[45]

Solar simulations were carried out with a Steuernagel Solarkonstant KHS1200 apparatus. Light intensity was adjusted to 100 mW cm^{-2} with a bolometric Zipp & Konen CM-4 pyranometer. The sun simulator was calibrated with a calibrated photodiode from Hamamatsu and a mini spectrophotometer from Ava-Spec 4200. The AM1.5G reference spectrum was agreed with the ASTM G173 standard. IV Curves were measured with a Keithley 2601 multimeter connected to a computer. IPCE analyses were carried out with a QE/IPCE measurement system from Oriel at 10 nm intervals from 300 to 600 nm. The IPCE equipment was calibrated before measurements with a S1227-1010BQ photodiode from Hamamatsu. The results were not corrected for intensity losses due to light absorption and reflection by the glass support.

Acknowledgments

The work described in this paper was supported by the Spanish National Plan of Research (CTQ2005-02808/PPQ and CTQ2008-00178/PPQ).

[1] Z. Y. Fan, J. G. Lu, *J. Nanosci. Nanotechnol.* **2005**, *5*, 1561–1573.
[2] S. J. Pearton, D. P. Norton, K. Ip, Y. W. Heo, T. Steiner, *Prog. Mater. Sci.* **2005**, *50*, 293–340.
[3] H. Morkoç, Ü. Özgür, *Zinc Oxide: Fundamentals, Materials and Device Technology*, Wiley-VCH, Weinheim, Germany, **2009**.
[4] Ü. Özgür, D. Hofstetter, H. Morkoç, *Proceedings of the IEEE*, **2010**, *98*, 1255–1268.
[5] Ü. Özgür, Y. I. Alivov, C. Liu, A. Teke, M. A. Reshchikov, S. Dogan, V. Avrutin, S. J. Cho, H. Morkoç, *J. Appl. Phys.* **2005**, *98*, 041301.
[6] B. Xu, Z. S. Cai, W. M. Wang, F. Y. Ge, *Surf. Coat. Technol.* **2010**, *204*, 1556–1561.
[7] Y. Saito, T. Shiga, A. Kokubun, T. Kawai, H. Unuma, *J. Ceram. Soc. Jpn.* **2007**, *115*, 938–940.
[8] J. J. Wu, S. C. Liu, *Adv. Mater.* **2002**, *14*, 215–218.
[9] S. Baruah, C. Thanachayanont, J. Dutta, *Sci. Technol. Adv. Mater.* **2008**, *9*, 025009.
[10] P. K. Arcot, J. Luo, *Surf. Coat. Technol.* **2008**, *202*, 2690–2697.
[11] A. Famengo, S. Anantharaman, G. Ischia, V. Causin, M. M. Natile, C. Maccato, E. Tondello, H. Bertagnolli, S. Gross, *Eur. J. Inorg. Chem.* **2009**, 5017–5028.
[12] D. Domide, E. Kaifer, J. Mautz, O. Walter, S. Behrens, H. J. Himmel, *Eur. J. Inorg. Chem.* **2008**, 3177–3185.
[13] M. Ortega-Lopez, A. Avila-Garcia, M. L. Albor-Aguilera, V. M. Sanchez-Resendiz, *Mater. Res. Bull.* **2003**, *38*, 1241–1248.
[14] X. F. Han, R. Liu, W. X. Chen, Z. D. Xu, *Thin Solid Films* **2008**, *516*, 4025–4029.
[15] G. Hodes, *Phys. Chem. Chem. Phys.* **2007**, *9*, 2181–2196.
[16] H. Parikh, M. R. De Guire, *J. Ceram. Soc. Jpn.* **2009**, *117*, 228–235.
[17] M. Yoshimura, R. Gallage, *J. Solid State Electrochem.* **2008**, *12*, 775–782.
[18] T. V. Richter, F. Stelzl, J. Schulz-Gericke, B. Kerscher, U. Wurfel, M. Niggemann, S. Ludwigs, *J. Mater. Chem.* **2010**, *20*, 874–879.
[19] D. Hariskos, S. Spiering, M. Powalla, *Thin Solid Films* **2005**, *480*, 99–109.
[20] I. Gonzalez-Valls, M. Lira-Cantu, *Energy Environ. Sci.* **2009**, *2*, 19–34.
[21] I. Gonzalez-Valls, M. Lira-Cantu, *Energy Environ. Sci.* **2010**, *3*, 789–795.
[22] M. S. White, D. C. Olson, S. E. Shaheen, N. Kopidakis, D. S. Ginley, *Appl. Phys. Lett.* **2006**, *89*, 143517.
[23] G. Dennler, K. Forberich, T. Ameri, C. Waldauf, P. Denk, C. J. Brabec, K. Hingerl, A. J. Heeger, *J. Appl. Phys.* **2007**, *102*, 123109.
[24] J. Y. Kim, K. Lee, N. E. Coates, D. Moses, T. Q. Nguyen, M. Dante, A. J. Heeger, *Science* **2007**, *317*, 222–225.
[25] J. Gilot, I. Barbu, M. M. Wienk, R. A. J. Janssen, *Appl. Phys. Lett.* **2007**, *91*, 113520.
[26] F. C. Krebs, *Sol. Energy Mater.* **2008**, *92*, 715–726.
[27] F. Verbakel, S. C. J. Meskers, R. A. J. Janssen, *J. Appl. Phys.* **2007**, *102*, 083701.
[28] F. Verbakel, S. C. J. Meskers, R. A. J. Janssen, *J. Phys. Chem. C* **2007**, *111*, 10150–10153.
[29] L. Schmidt-Mende, J. L. MacManus-Driscoll, *Mater. Today* **2007**, *10*, 40–48.
[30] C. J. Brabec, J. A. Hauch, P. Schilinsky, C. Waldauf, *MRS Bull.* **2005**, *30*, 50–52.
[31] H. J. Bolink, E. Coronado, M. Sessolo, *Chem. Mater.* **2009**, *21*, 439–441.
[32] D. G. Yoo, S. H. Nam, M. H. Kim, S. H. Jeong, H. G. Jee, H. J. Lee, N. E. Lee, B. Y. Hong, Y. J. Kim, D. Jung, J. H. Boo, *Surf. Coat. Technol.* **2008**, *202*, 5476–5479.
[33] K. Ghule, A. V. Ghule, B. J. Chen, Y. C. Ling, *Green Chem.* **2006**, *8*, 1034–1041.
[34] Y. Yu, Z. H. Jiang, G. Wang, Y. Song, *Holzforschung* **2010**, *64*, 385–390.
[35] D. Yuvaraj, R. Kaushik, K. N. Rao, *ACS Appl. Mater. Interf.* **2010**, *2*, 1019–1024.
[36] I. Perelshtein, G. Applerot, N. Perkas, E. Wehrschetz-Sigl, A. Hasmann, G. M. Guebitz, A. Gedanken, *ACS Appl. Mater. Interf.* **2009**, *1*, 363–366.
[37] N. A. Ibrahim, M. Gouda, S. M. Husseiny, A. R. El-Gamal, F. Mahrous, *J. Appl. Polym. Sci.* **2009**, *112*, 3589–3596.
[38] H. Gullapalli, V. S. M. Vemuru, A. Kumar, A. Botello-Mendez, R. Vajtai, M. Terrones, S. Nagarajaiah, P. M. Ajayan, *Small* **2010**, *6*, 1641–1646.
[39] L. S. Skogareva, N. A. Minaeva, T. V. Filippova, *Russ. J. Inorg. Chem.* **2009**, *54*, 1341–1349.
[40] S. T. Meyers, J. T. Anderson, C. M. Hung, J. Thompson, J. F. Wager, D. A. Keszler, *J. Am. Chem. Soc.* **2008**, *130*, 17603–17609.
[41] J. Saussey, J. C. Lavalley, C. Bovet, *J. Chem. Soc., Faraday Trans. 1* **1982**, *78*, 1457–1463.
[42] Z. W. Pan, J. Tao, Y. M. Zhu, J. F. Huang, M. P. Paranthaman, *Chem. Mater.* **2010**, *22*, 149–154.
[43] X. Z. Liu, Y. H. Luo, H. Li, Y. Z. Fan, Z. X. Yu, Y. Lin, L. Q. Chen, Q. B. Meng, *Chem. Commun.* **2007**, 2847–2849.
[44] L. M. Peter, *Phys. Chem. Chem. Phys.* **2007**, *9*, 2630–2642.
[45] S. Brunauer, P. H. Emmett, E. Teller, *J. Am. Chem. Soc.* **1938**, *60*, 309–319.

Received: September 9, 2010
Published Online: January 12, 2011

